Available online at www.sciencedirect.com
ScienceDirect
Phytochemistry 68 (2007) 464–477
PHYTOCHEMISTRY
www.elsevier.com/locate/phytochem

Catalytic implications of the higher plant ADP-glucose pyrophosphorylase large subunit

Seon-Kap Hwang [a], Shigeki Hamada [a,b], Thomas W. Okita [a,*]

[a] *Institute of Biological Chemistry, Washington State University, Pullman, WA 99164-6340, USA*
[b] *Division of Applied Bioscience, Graduate School of Agriculture, Hokkaido University, Sapporo 060-8589, Japan*

Received 27 July 2006; received in revised form 23 October 2006
Available online 4 January 2007

Abstract

ADP-glucose pyrophosphorylase, a key regulatory enzyme of starch biosynthesis, is composed of a pair of catalytic small subunits (SSs) and a pair of catalytically disabled large subunits (LSs). The N-terminal region of the LS has been known to be essential for the allosteric regulatory properties of the heterotetrameric enzyme. To gain further insight on the role of this region and the LS itself in enzyme function, the six proline residues found in the N-terminal region of the potato tuber AGPase were subjected to scanning mutagenesis. The wildtype and various mutant heterotetramers were expressed using our newly developed host-vector system, purified, and their kinetic parameters assessed. While $P_{17}L$, $P_{26}L$, and $P_{55}L$ mutations only moderately affected the kinetic properties, $P_{52}L$ and $P_{66}L$ gave rise to significant and contrasting changes in allosteric properties: $P_{66}L$ enzyme displayed up-regulatory properties toward 3-PGA while the $P_{52}L$ enzyme had down-regulatory properties. Unlike the other mutants, however, various mutations at P_{44} led to only moderate changes in regulatory properties, but had severely impaired catalytic rates, apparent substrate affinities, and responsiveness to metabolic effectors, indicating Pro-44 or the LS is essential for optimal catalysis and activation of the AGPase heterotetramer. The catalytic importance of the LS is further supported by photoaffinity labeling studies, which revealed that the LS binds ATP at the same efficiency as the SS. These results indicate that the LS, although considered having no catalytic activity, may mimic many of the catalytic events undertaken by the SS and, thereby, influences net catalysis of the heterotetrameric enzyme.

Keywords: Potato tuber AGPase; ADP-glucose pyrophosphorylase; Large subunit; Allosteric regulation; Catalytic roles; *In vitro* mutagenesis; Photoaffinity labeling

1. Introduction

ADP-glucose pyrophosphorylase (EC 2.7.7.27; AGPase) catalyzes a pivotal reaction in controlling carbon flux in the α-glucan (starch/glycogen) pathway in plants and bacteria (Preiss, 1984; Preiss et al., 1991; Slattery et al., 2000; Ballicora et al., 2004). While the AGPases from enteric bacteria are activated by fructose-1,6-diphosphate and inhibited by AMP, the enzymes from plants and some photosynthetic algae are activated and inhibited by the major photosynthetic metabolites 3-PGA and inorganic phosphate (Pi), respectively. These regulatory properties are not ubiquitous as the major seed enzyme activities from wheat (Gomez-Casati and Iglesias, 2002) and barley (Kleczkowski et al., 1993a,b; Doan et al., 1999) are relatively unresponsive to these effectors.

Despite possessing similar catalytic and allosteric regulatory properties, the bacterial and higher plant enzymes have different structures. AGPases from bacteria and cyanobacteria are homotetrameric in composition consisting of a single subunit type (α_4), whereas the enzymes from plants have a $\alpha_2\beta_2$ structure comprised of a pair of large subunits (LSs) and a pair of small subunits (SSs) (Iglesias et al., 1993). The subunit types appeared to play different roles in enzyme function. In the absence of the LSs, the

* Corresponding author. Tel.: +1 50 933 53391; fax: +1 50 933 57643.
E-mail address: okita@wsu.edu (T.W. Okita).

0031-9422/$ - see front matter © 2006 Published by Elsevier Ltd.
doi:10.1016/j.phytochem.2006.11.027

SSs are capable of self-assembly into bacterial-like (S_4) AGPases. While the catalytic activity of the potato tuber S_4 is still regulated by effector molecules, it displays significant reduction in 3-PGA sensitivity and increased sensitivity to Pi inhibition (Ballicora et al., 1995; Salamone et al., 2000). Although possessing a related primary sequence, the potato tuner LSs are incapable of efficient self-assembly into a catalytically active oligomeric enzyme (Iglesias et al., 1993; Doan et al., 1999). The presence of the LSs enhances the allosteric properties of the heterotetrameric enzyme suggesting that the LS is a regulatory subunit. This functional assignment was supported by results from a photoaffinity labeling studies using pyridoxal 5-phosphate, which mimics 3-PGA in activating the enzyme. The potato tuber LS was preferentially labeled at three sites whereas the SS was labeled at a single site (Ball and Preiss, 1994). However, site directed mutagenesis of the putative lysine residues located at or near the 3-PGA activator binding site in the SS markedly reduced sensitivity to 3-PGA compared to corresponding mutations in the LS (Ballicora et al., 1998). This result suggested that the LS was not a regulatory subunit in providing the effector binding sites but, instead, served as a modulator in affecting the allosteric regulatory properties of the catalytic SS (Ball and Preiss, 1994; Ballicora et al., 1995, 1998; Greene et al., 1996a,b; Laughlin et al., 1998; Kavakli et al., 2001). Several point mutations in the SS also drastically enhanced the up-regulatory properties of the heterotetrameric enzyme supporting the dominant role of this subunit (Salamone et al., 2000; Salamone et al., 2002). Results from other studies (Cross et al., 2004; Hwang et al., 2005), however, do not support this narrow functional assignments for the LS and SS. Analysis of maize-potato mosaics of AGPase indicated that both subunit types contributed to regulatory properties (Cross et al., 2004). This view was also supported by the analysis of AGPase enzymes containing various combinations of wildtype and mutant LSs and SSs (Hwang et al., 2005). The net regulatory properties of enzymes containing different combinations of up-regulatory and down-regulatory LSs and SSs were significantly higher than the combined properties of each subunit type, indicating that the two subunits interact synergistically. Thus, both subunits contribute to the allosteric regulatory properties of the heterotetrameric enzyme.

Available evidence indicates that the N-terminal region of the potato tuber LS plays a major role in specifying the enzyme's allosteric regulatory properties. Deletion of the first 17 amino acids of the LS gave rise to marked increases both in sensitivity to 3-PGA and in resistance to Pi inhibition with little change in catalytic properties (Laughlin et al., 1998). Further deletion of 11 additional amino acid residues reversed the effect of the smaller 17 amino acid deletion. The deletion mutant showed roughly unchanged substrate affinities and 3-PGA sensitivity from the wildtype condition. Random mutagenesis studies showed that a single mutation at Glu-38 or Pro-52 in the LS (designated $E38^{LS}$ or $P52^{LS}$) significantly altered the allosteric behaviors of the AGPase. $E_{38}K^{LS}$ resulted in an enzyme with enhanced sensitivity to 3-PGA activation and enhanced resistance to Pi inhibition (up-regulatory phenotype) while $P_{52}L^{LS}$ rendered the enzyme with the opposite down-regulatory phenotype (Greene et al., 1996a,b, 1998; Hwang et al., 2005).

In this study, we employed a leucine-scanning mutagenesis to further investigate the role of the N-terminal region of the potato tuber LS in the enzyme function of AGPase. Pro were selected for mutagenesis as this residue has restricted conformational flexibility and hence its replacement is likely to cause significant changes in structure and, in turn, protein function and stability (Reiersen and Rees, 2001). Structural and kinetic analyses indicate that mutations of three proline residues located between residues 44 and 66 dramatically alter enzyme function, each having distinct effects on allosterism or catalysis. Replacement of $P52^{LS}$ and $P66^{LS}$ produced enzymes with down- and up-regulatory properties, respectively. Interestingly, $P44^{LS}$ is critical for catalytic activity, substrate affinities, and responsiveness to metabolic effectors. We also show that the LS is labeled by 8-azido-ATP, a substrate analog, at a level comparable to SS. This empirical result implicates a more direct involvement of the non-catalytic LS in the formation of ADP-glucose by the heterotetramer AGPase.

2. Results

2.1. New host cell and plasmids for AGPase expression

During the course of our studies on AGPase, efforts were continually directed at improving the expression of the recombinant enzymes. Production of recombinant AGPase has relied on the *glgC*-deficient strain AC70R1-504 (Ballicora et al., 1995) which has been used for the expression of several plant AGPases. Despite the general utility of this host strain, it contains active protease activities which not only can significantly reduce net AGPase activity but could also potentially modify the enzyme's properties (Salamone et al., 2000). These features prompted us to generate a new host strain lacking both protease and endogenous AGPase activities. The *Escherichia coli* strain ER2566 was selected to generate a *glgC* null mutation because this strain lacks the major protease activities (*lon* and *ompT*) as well as the endonuclease A (*endA*), which aids in plasmid stability. The *E. coli* AGPase structural gene *glgC* was inactivated using the pKO-1 recombination system (Link et al., 1997) which inserted a 0.72 kb fragment of bacteriophage λ DNA into the N-terminal coding sequence of the gene to yield strain EA345 (Fig. 1a).

A potential complication in the study of the heterotetrameric AGPase mutants is the contamination from homotetrameric enzyme forms, a serious problem in those cells which preferentially express the SS compared to the LS due to differences in promoter strength. To minimize this

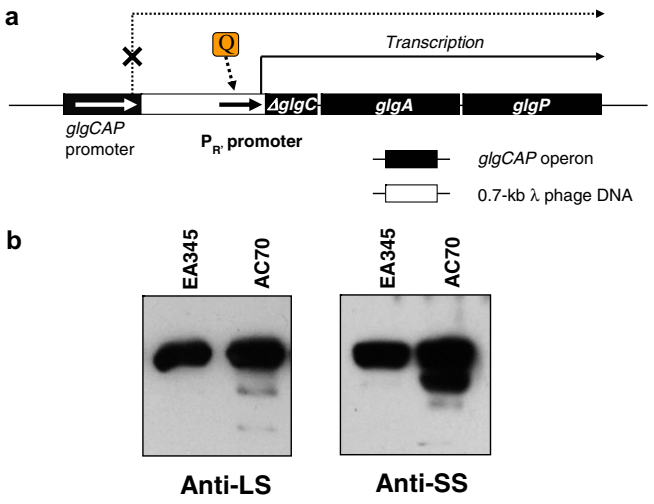

Fig. 1. Expression of AGPase in *E. coli* host cells. (a) Schematic diagram of the *glgC* null mutation of *glgCAP* operon in EA345 cells. Lambda Q gene product (from pSH228) is required for initiating transcription of *glgA* and *glgP* genes. (b) Immunoblot analysis of AGPase expressed in AC70R1-504 and EA345 cells was carried out using antibodies raised against the potato large subunit (Anti-LS) or the small subunit (Anti-SS). Five μg of the crude cell extracts were used for 12% SDS–PAGE.

potential problem, two new plasmids pSH275 (LS) and pSH228 (SS) were constructed to express the AGPase subunits. These new plasmids have several advantages over pML7 and pML10, which have been routinely used for co-expression of the AGPase subunits. Expression of the AGPase subunits can now be activated with a single inducer, IPTG, thus avoiding the toxic nalidixic acid, which was used to induce expression under the *recA* promoter in pML7. Moreover, expression of the enzyme is more tightly controlled by the LacI repressor produced from pSH228. This plasmid also contained the Q gene which activates the lambda $P_{R'}$ promoter and enables transcription of downstream genes, *glgA* (glycogen synthase structural gene) and *glgP*, of the *glg* operon and restoration of glycogen production in the presence of AGPase (Fig. 1a).

Plasmids pSH275 and pSH228 were introduced into AC70R1 or EA345 cells and expressed. Crude cell extracts of both transformants were prepared and analyzed by using immunoblot analysis (Fig. 1b). In contrast to the partially degraded enzyme isolated from AC70R1, the enzyme produced in the EA345 cells was largely intact.

2.2. Generation and expression of the proline mutant enzymes

The AGPase LS contains six Pro residues within the first 66 residues of the N-terminal region (Fig. 2a). $P17^{LS}$ is only moderately conserved among plant AGPases while the other five remaining residues ($P26^{LS}$ to $P66^{LS}$) are strongly conserved among plant AGPase subunits. $P17^{LS}$, $P26^{LS}$, $P52^{LS}$, and $P55^{LS}$ are predicted to be located in flexible loops (Fig. 2a and b). $P44^{LS}$ is in the loop located between the glycine-rich region (residues 36–42, GGEGTKL), important for positioning of the ATP phosphates groups (Jin et al., 2005) and the strongly conserved "PAV" region (residues 52–54) associated with both catalysis and allosteric control, whereas $P66^{LS}$ lies in a helix. These Pro residues were individually mutated to Leu by site-directed mutagenesis (Table 1) and then co-expressed with wildtype SS in EA345 cells. The effect of these mutations on AGPase activity was qualitatively determined *in vivo* by assessing the level of glycogen by iodine staining in the various mutant lines (Fig. 2c). Cells expressing enzyme variants containing $P_{17}L$, $P_{55}L$, and $P_{66}L$ showed similar glycogen levels as wildtype, while those expressing $P_{26}L$ and $P_{52}L$ accumulated significantly lower amounts. Interestingly, cells expressing $P_{44}L$ variant enzyme produced little, if any, glycogen.

2.3. Implications of proline residues on ADP-glucose pyrophosphorylase properties

Our previous results showed that attachment of the polyhistidine sequence to the N-terminus of the LS expedited the rapid purification of near homogeneous AGPases, without having any effect on enzyme kinetics (Hwang et al., 2004). Purification of the AGPase variants was accomplished using successive DEAE ion exchange and immobilized metal affinity chromatography (IMAC). An additional purification step using Butyl-Sepharose Fast Flow column was also performed to obtain intact, near homogeneous enzyme samples (purity > 95%). Table 2 shows the allosteric properties of the variant AGPases as well as wildtype enzyme. Consistent with results from a previous study (Hwang et al., 2005), $P_{52}L$ required 7-fold greater amounts of 3-PGA for 50% activation ($A_{0.5}$) than wildtype enzyme. In contrast, $P_{66}L$ showed up-regulatory properties with about a 3-fold increase in sensitivity to 3-PGA and corresponding increase in resistance to Pi inhibition. With the exception of $P_{17}L$ which showed a slight decrease in $A_{0.5}$, the remaining Pro mutants showed only moderate increases in $A_{0.5}$ values.

All of the Pro mutations with the exception of $P_{44}L$ had apparent substrate affinity values for ATP and Glc-1-P roughly similar (<2-fold) to the wildtype enzyme (Table 2). $P_{44}L$, however, showed significant changes in apparent substrate affinities, about 3.6-fold decrease for ATP and 7-fold decrease for Glc-1-P. $P_{44}L$ mutation also severely affected net catalytic activity. While the other mutations moderately decreased the apparent catalytic rate (K_{cat}, 3-fold or less), the $P_{44}L$ mutation reduced the catalytic rate to less than 3% of wildtype. It is also interesting to note that when the apparent K_{cat} values are plotted against the distance from the N-terminus, the $P_{44}L$ mutation lies in a trough with the catalytic activity increasing towards the C-terminal (i.e. $P_{44}L < P_{52}L < P_{55}L$, $P_{66}L$). The catalytic efficiencies ($K_{cat}/S_{0.5}$) showed even greater differences between wildtype and $P_{44}L$ mutant: $P_{44}L$ mutant showed 126-fold and 267-fold lower catalytic efficiencies for ATP and Glc-1-P, respectively, compared to wildtype. These results indicate that LS's N-terminal region and, specifi-

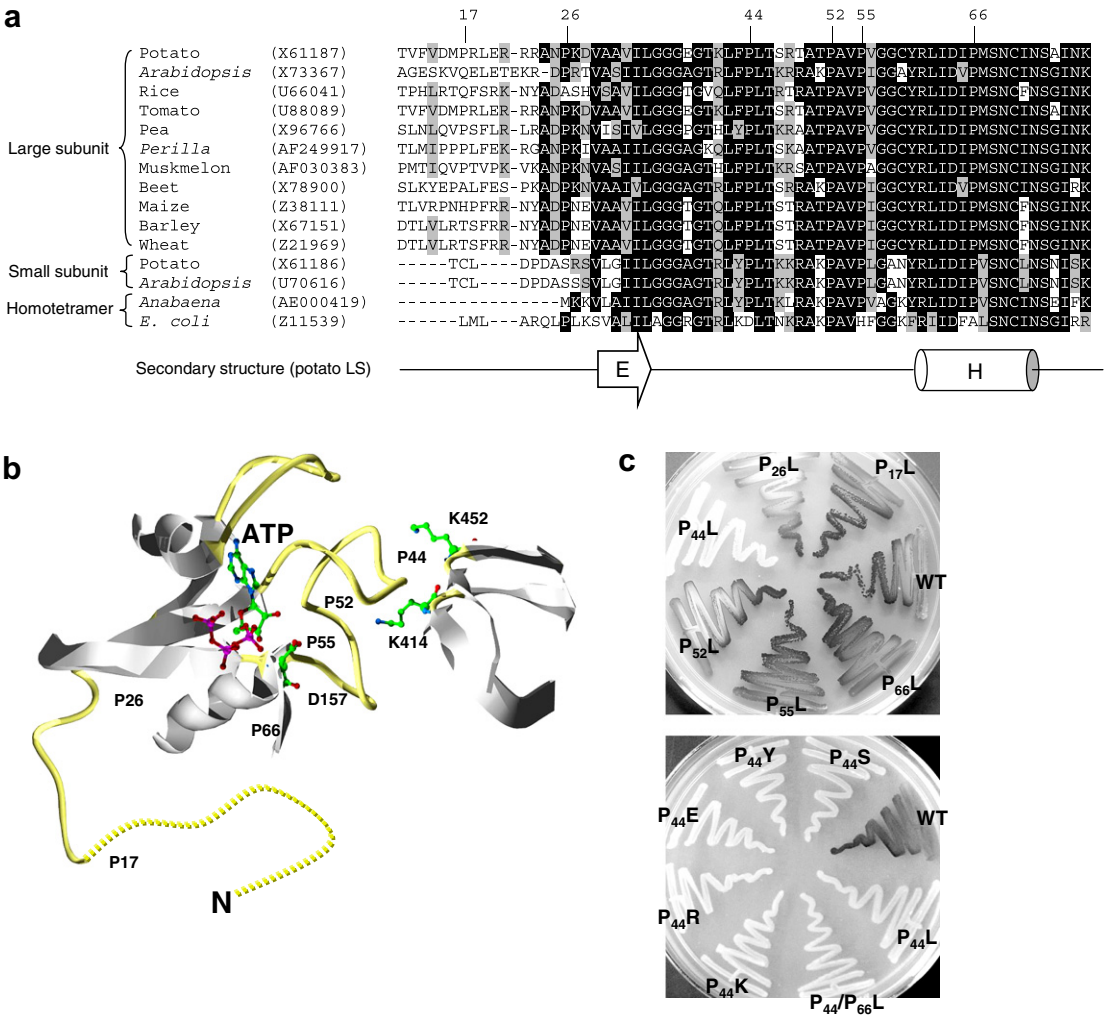

Fig. 2. (a) Amino acid sequence alignment (residues 11–73) for AGPases. GenBank accession numbers are in parentheses. Proline residues are numbered based on the recombinant form of the potato large subunit (X61187) (Greene et al., 1998); the two additional amino acids at the N-terminus in the recombinant form were excluded. Identical residues and similar residues are shaded in black and gray, respectively. Deletions in the sequences are indicated by a dash. The helical structure is shown with a cylinder (H), β-sheet with an arrow (E), and coiled structure with a line. Only the secondary structures with more than 50% of confidence level calculated by PSIPRED protein structure prediction server (McGuffin et al., 2000) are presented. (b) Modeled structure of the potato AGPase LS. Only the N-terminal region containing the putative ATP binding site (residues 18–73, 107–134, and 149–159), and the regions (residues 407–419 and 446–455) containing the putative 3-PGA binding sites ($K414^{LS}$ and $K452^{LS}$) of the LS were modeled by comparison with the known structure of the potato AGPase SS (PDB 1yp3). The modeled position of ATP is shown. The α-helix and β-sheet are colored in gray and the loop in yellow. Proline residues and some important residues in the LS are indicated by red arrowheads with their location numbers. Oxygen is depicted in red, nitrogen in blue, carbon in green, and phosphate in pink. The residues 1–17 of the LS are shown as a dotted line because structural information on the SS is not available for comparison/prediction. The $P17^{LS}$ and $P26^{LS}$ precede the ATP binding site, while $P44^{LS}$, $P52^{LS}$, and $P55^{LS}$ are located in the loop structure next to the binding site. $P66^{LS}$ is located in the helical structure. Note that the predicted P-loop structure (from residue 35 to 42) is very close to $P44^{LS}$. (c) Iodine staining of the *E. coli* EA345 cells expressing various LS proline mutants with wildtype SS.

cally $P44^{LS}$, are essential for the catalytic properties of AGPase. However, our circular dichroism analysis did not reveal significant differences between the wildtype and mutant AGPases (Fig. 3). This indicates that the mutations including $P_{44}L$ have little, if any, effect on the overall conformation of the proteins.

2.4. Kinetic properties of $P44^{LS}$ mutants

The effect of the nature of the amino acid residue at $P44^{LS}$ on the kinetic properties of the AGPase was further examined (Table 3). Since a mutation of $E38^{LS}$ to K38, which is only six amino acids removed from $P44^{LS}$, led to an up-regulatory AGPase (Greene et al., 1998), we hypothesized that replacement of the $P44^{LS}$ with different amino acids might affect the allosteric properties of the enzyme. Using site-directed mutagenesis, $P44^{LS}$ residue was replaced with Lys ($P_{44}K$), Arg ($P_{44}R$), Glu ($P_{44}E$), Tyr ($P_{44}Y$), or Ser ($P_{44}S$), residues which differ in net charge and R group. When the mutants were co-expressed with wildtype SS, none of the *E. coli* cells expressing these various mutant AGPases showed detectable iodine staining (Fig. 2c), indicating that they were similar in net properties as the $P_{44}L$ enzyme. Kinetic analysis also showed that

Table 1
Oligonucleotide primers used in this study

Name	Sequence[a]	Restriction site
5′glgc S	5′GCTCTCCCCGGGTACGCCGATGTTACT3′	*Sma*I
5′glgc AS	5′CTCTAAACTAACCATGGCTAACTCCTT3′	*Nco*I
glgc S	5′AAGGAGTTAGCCATGGTTAGTTTAGAG3′	*Nco*I
pyro7	5′GATCACACAACCGCCGGAAACCAGTGA3′	
Q-Ncmut-F	5′ TGCAGAGATTGCCACGGTACAGGCCGTG 3′	
Q-Ncmut-R	5′ CACGGCCTGTACCGTGGCAATCTCTGCA 3′	
LP17L-F	5′ACTGTGTTCGTAGATATG**CTC**CGTCTTGAGAGACGCCGG3′	
LP17L-R	5′CCGGCGTCTCTCAAGACG**GAG**CATATCTACGAACACAGT3′	
LP26L-F	5′GAGAGACGCCGGGCAAAT**CTC**AAGGATGTGGCTGCAGTC3′	
LP26L-R	5′GACTGCAGCCACATCCTT**GAG**ATTTGCCCGGCGTCTCTC3′	
LP44L-F	5′GAAGGGACCAAGTTATTC**CTC**CTTACAAGTAGAACTGCA3′	
LP44L-R	5′TGCAGTTCTACTTGTAAG**GAG**GAATAACTTGGTCCCTTC3′	
LP55L-F	5′ACTGCAACCCCTGCTGTT**CTC**GTTGGAGGATGCTACAGG3′	
LP55L-R	5′CCTGTAGCATCCTCCAAC**GAG**AACAGCAGGGGTTGCAGT3′	
LP66L-F	5′TACAGGCTAATAGACATC**CTC**ATGAGCAACTGTATCAAC3′	
LP66L-R	5′GTTGATACAGTTGCTCAT**GAG**GATGTCTATTAGCCTGTA3′	
LP44K-F	5′GAAGGGACCAAGTTATTC**AAA**CTTACAAGTAGAACTGCA3′	
LP44K-F	5′TGCAGTTCTACTTGTAAG**TTT**GAATAACTTGGTCCCTTC3′	
LP44R-F	5′GAAGGGACCAAGTTATTC**CGC**CTTACAAGTAGAACTGCA3′	
LP44R-R	5′TGCAGTTCTACTTGTAAG**GCG**GAATAACTTGGTCCCTTC3′	
LP44E-F	5′GAAGGGACCAAGTTATTC**GAA**CTTACAAGTAGAACTGCA3′	
LP44E-R	5′TGCAGTTCTACTTGTAAG**TTC**GAATAACTTGGTCCCTTC3′	
LP44Y-F	5′GAAGGGACCAAGTTATTC**TAT**CTTACAAGTAGAACTGCA3′	
LP44Y-R	5′TGCAGTTCTACTTGTAAG**ATA**GAATAACTTGGTCCCTTC3′	
LP44S-F	5′GAAGGGACCAAGTTATTC**AGC**CTTACAAGTAGAACTGCA3′	
LP44S-R	5′TGCAGTTCTACTTGTAAG**GCT**GAATAACTTGGTCCCTTC3′	

[a] Restriction enzyme recognition sites are underlined. The mutated sequences are in boldface.

Table 2
Allosteric and catalytic parameters of the recombinant wildtype and mutant heterotetrameric AGPases

Enzyme	Wildtype	$P_{17}L$	$P_{26}L$	$P_{44}L$	$P_{52}L$	$P_{55}L$	$P_{66}L$
Kinetic parameter							
$A_{0.5}$ (mM) for 3-PGA	0.11 (1.0[a])	0.08 (1.0)	0.15 (1.4)	0.25 (1.1)	0.77 (1.2)	0.26 (1.6)	0.03 (1.0)
$I_{0.5}$ (mM) at							
0.05 mM 3-PGA	0.06 (0.9)	0.11 (1.1)	0.07 (1.4)	ND[b]	0.20 (0.9)	0.08 (1.1)	0.14 (0.9)
0.5 mM 3-PGA	0.34 (1.1)	0.59 (1.1)	0.22 (1.5)	0.27 (1.0)	0.24 (1.0)	0.53 (1.0)	1.56 (1.0)
5 mM 3-PGA	2.14 (1.4)	3.04 (1.2)	1.32 (1.1)	0.88 (0.9)	1.58 (1.0)	3.02 (1.0)	8.46 (1.1)
$S_{0.5}$ (mM)							
ATP	0.19 (1.2)	0.21 (1.2)	0.14 (1.3)	0.68 (1.2)	0.27 (1.1)	0.33 (1.6)	0.20 (1.3)
Mg^{2+}	2.4 (4.0)	2.3 (3.9)	2.8 (3.9)	2.9 (2.8)	2.3 (2.8)	3.4 (4.1)	2.0 (2.7)
Glc-1-P	0.12 (1.1)	0.16 (1.4)	0.09 (1.4)	0.83 (1.0)	0.15 (1.1)	0.14 (1.2)	0.14 (1.3)
K_{cat} (s^{-1})	96	62	67	2.7	33	49	72
Catalytic efficiency[c]							
ATP	505	295	479	4	122	148	360
Glc-1-P	800	388	744	3	220	350	514

All values were determined from ADP-glucose synthesis assay (Assay B, see Section 5) data of at least two iterations, and the SE was <15% in all cases. When the SE value was greater than 10%, further two reactions were performed to obtain reliable data. The mean values are presented here. The $I_{0.5}$ value was obtained by performing the reactions at 37 °C for 10 min in the presence of varied 3-PGA concentrations (0.05, 0.5, and 0.5 mM). Calculation method for the $A_{0.5}$, $I_{0.5}$, and *n*H values were described in Section 5. The apparent $S_{0.5}$ and K_{cat} for ATP, Mg^{2+}, and Glc-1-P were obtained under the saturating condition where 5 mM 3-PGA was added.

[a] Hill coefficient (*n*H).

[b] Not determined.

[c] $K_{cat}/S_{0.5}$ (s^{-1} M^{-1}), $\times 10^3$.

irrespective of the amino acid type, the 3-PGA activation profiles of the various $P44^{LS}$ mutants were very similar to that of the $P_{44}L$ mutant (Table 3) and all of the $P44^{LS}$ mutants had intermediate levels of 3-PGA sensitivity ranging between wildtype AGPase and $P_{52}L$ mutant, i.e. the $A_{0.5}$ values for the $P44^{LS}$ mutants were between 0.2 mM to 0.35 mM. The mutants also showed similar $I_{0.5}$ profiles with the $P_{44}L$ mutant for resistance against Pi inhibition. The substrate affinities still remained low with only a slight amount of variation noted. Only a 2- to 3-fold increase in

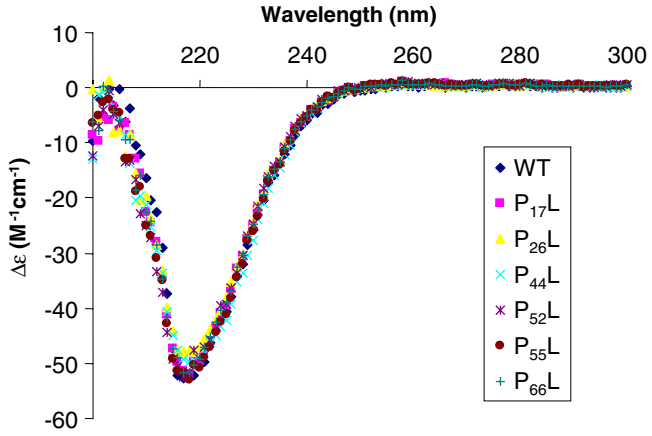

Fig. 3. CD spectra of the wildtype and mutant AGPases.

the apparent K_{cat} values were observed for the various P44^{LS} mutants compared to the P_{44}L mutant. The catalytic efficiencies still remained very low compared to the wildtype (less than 2.5% for ATP and 1.2% for Glc-1-P).

2.5. Responses of the proline mutants to metabolites

Since several of the Pro mutants showed varying sensitivity to the activator 3-PGA (Tables 2 and 3), the responses of these various enzymes to different metabolites were investigated (Table 4). Wildtype AGPase showed the highest fold-activation (V_a/V_o) by 3-PGA (31-fold), intermediate responses by 2-PGA (15-fold), PEP (14-fold), and fructose-6-phosphate (10-fold), and lower levels by glucose-6-phosphate and AMP (4-fold). Thus these metabolites may serve to activate AGPase under physiological conditions. However, sugars containing two acidic groups such as glucose-1,6-bisphosphate and fructose-1,6-bisphosphate as well as pyruvate were poor activators for AGPase.

P_{17}L showed slightly reduced fold-activation to all effectors used in this study. While the extent of activation of P_{26}L by 3-PGA was unchanged, it showed significantly lowered responsiveness to 2-PGA (4.4-fold). The responsiveness of the enzyme to these various effectors was further impaired by the P_{44}L mutation (7-fold decrease for 3-PGA, 10-fold for 2-PGA, 3-fold for PEP, and 5-fold for fructose-6-phosphate). However, mutations distal to P44^{LS} did not show pronounced decrease in the fold-activation by 3-PGA, although reduction was evident for 2-PGA and other effectors. Since the P_{44}L mutation drastically lowered the responsiveness of the enzyme to various metabolic effectors, we also determined the fold-activations of the various P44^{LS} mutants. Irrespective of the nature of the amino acid replacement, all of the P44^{LS} mutants showed activation patterns similar to that observed for P_{44}L (Table 4). These observations indicate that P44^{LS} is essential for responsiveness of AGPase to metabolic effectors.

2.6. Photoaffinity labeling of the AGPase heterotetramers

Kinetic results in Tables 2 and 3 of the wildtype and proline mutants suggest that the N-terminal region of the LS is closely associated with enzyme catalysis. Mutations at P44^{LS} significantly impaired enzyme's catalytic properties, especially substrate affinities of AGPase. In addition, P44^{LS} resides near the ATP binding glycine-rich residues (Fig. 2a and b). Thus a photoaffinity labeling experiment using [α^{32}P]8-N_3ATP was conducted to see the apparent ATP binding affinities of the wildtype and P_{44}L mutant AGPases.

This analog served as a substrate with a similar $S_{0.5}$ (0.23 mM vs. 0.19 mM for ATP) when assayed with wildtype AGPase under non-labeling conditions. Incubation of the enzyme with non-isotopic 8-N_3ATP (1.2 mM) under

Table 3
Allosteric and catalytic parameters of the P44^{LS} mutants

Enzyme	Wildtype	P_{44}L	P_{44}K	P_{44}R	P_{44}E	P_{44}Y	P_{44}S
Kinetic parameter							
$A_{0.5}$ (mM) for 3-PGA	0.11 (1.0[a])	0.25 (1.1)	0.20 (1.0)	0.21 (1.2)	0.33 (1.1)	0.25 (1.2)	0.35 (1.0)
$I_{0.5}$ (mM) at							
0.05 mM 3-PGA	0.06 (0.9)	ND[b]	ND	ND	ND	ND	ND
0.5 mM 3-PGA	0.34 (1.1)	0.27 (1.0)	0.34 (1.2)	0.37 (0.9)	0.37 (1.1)	0.39 (0.9)	0.31 (1.1)
5 mM 3-PGA	2.14 (1.4)	0.88 (0.9)	1.38 (1.2)	1.69 (0.9)	0.92 (1.1)	1.09 (0.9)	0.90 (1.4)
$S_{0.5}$ (mM)							
ATP	0.19 (1.2)	0.68 (1.2)	0.67 (1.2)	0.66 (1.2)	0.77 (1.1)	0.88 (1.0)	0.62 (1.2)
Mg^{2+}	2.4 (4.0)	2.9 (2.8)	3.2 (2.7)	2.9 (3.3)	2.9 (2.7)	3.2 (3.2)	3.0 (2.9)
Glc-1-P	0.12 (1.1)	0.83 (1.0)	0.91 (1.4)	1.05 (1.4)	1.00 (1.0)	1.32 (1.1)	0.82 (1.2)
K_{cat} (s^{-1})	96	2.7	8.2	8.9	8.9	5.5	5.1
Catalytic efficiency[c]							
ATP	505	4	12	13	12	6	8
Glc-1-P	800	3	9	8	9	4	6

The statistical explanation and details on the experiment are same as described in Table 2.
[a] Hill coefficient (nH).
[b] Not determined.
[c] $K_{cat}/S_{0.5}$ (s^{-1} M^{-1}), $\times 10^3$.

Table 4
Responsiveness of the AGPases toward metabolic effectors

Enzyme	Wildtype	$P_{17}L$	$P_{26}L$	$P_{44}L$	$P_{52}L$	$P_{55}L$	$P_{66}L$	$P_{44}K$	$P_{44}R$	$P_{44}E$	$P_{44}Y$	$P_{44}S$
Metabolite[a]	Fold activation (V_a/V_o)[b]											
3-PGA	30.9	22.5	31.8	4.3	26.5	27.2	18.0	3.8	3.6	5.1	4.1	4.6
2-PGA	14.8	8.6	3.4	1.5	2.2	2.7	8.7	1.9	1.6	1.6	1.6	1.6
PEP	13.7	9.0	8.6	4.2	7.7	9.5	7.8	4.7	3.7	5.6	3.7	4.7
Glc-6-P	4.3	3.6	3.0	2.0	3.5	4.0	3.6	2.2	2.0	2.2	1.8	1.8
Glc-1,6-P	0.5	0.7	1.4	0.8	1.9	1.5	0.7	0.9	0.8	0.9	0.5	0.7
Fruc-6-P	9.8	6.5	5.0	1.9	3.1	3.7	7.1	2.5	2.2	2.2	1.4	1.9
Fruc-1,6-P	1.0	1.2	2.2	1.4	1.7	2.9	1.4	1.8	1.4	1.8	1.2	1.4
Pyruvate	0.4	0.8	1.2	1.1	0.6	2.4	1.1	1.1	0.8	1.0	0.7	0.9
AMP	4.5	2.9	3.1	1.5	3.6	3.6	3.3	1.7	1.5	1.8	1.2	1.6

All values were determined from ADP-glucose synthesis assay (Assay B, see Section 5). The statistical explanation and details on the experiment are presented in Table 2.

[a] 3-PGA, 3-phosphoglycerate; 2-PGA, 2-phosphoglycerate; PEP, phosphoenol pyruvate; Glc-6-P, glucose-6-phosphate; Glc-1,6-P, glucose-1,6-diphosphate; F-6-P, fructose-6-phoshate; F-1,6-P, fructose-1,6-diphosphate; AMP, adenosine 5′-monophosphate.

[b] The V_a values were obtained by performing the reactions at 37 °C for 10 min in the presence of 4 mM effectors while the V_o values were obtained in the absence of the effectors. Fold activation or responsiveness of the enzyme toward the effectors was calculated by V_a/V_o.

UV results in a near total loss (>95%) of enzyme activity (details not shown). As expected, when the wildtype enzyme was labeled, molecular size of the AGPase SS increased by incorporation of ^{32}P-ATP (Fig. 4a, first, second, and fourth rows). Interestingly, immunoblot analysis with a LS-specific antibody revealed that the molecular size of the LS was also increased significantly (Fig. 4a, third row), indicating that the LS is capable of interacting with ATP. The stoichiometry for 8-N_3ATP labeling of the AGPase subunits was also studied at a sub-saturating con-

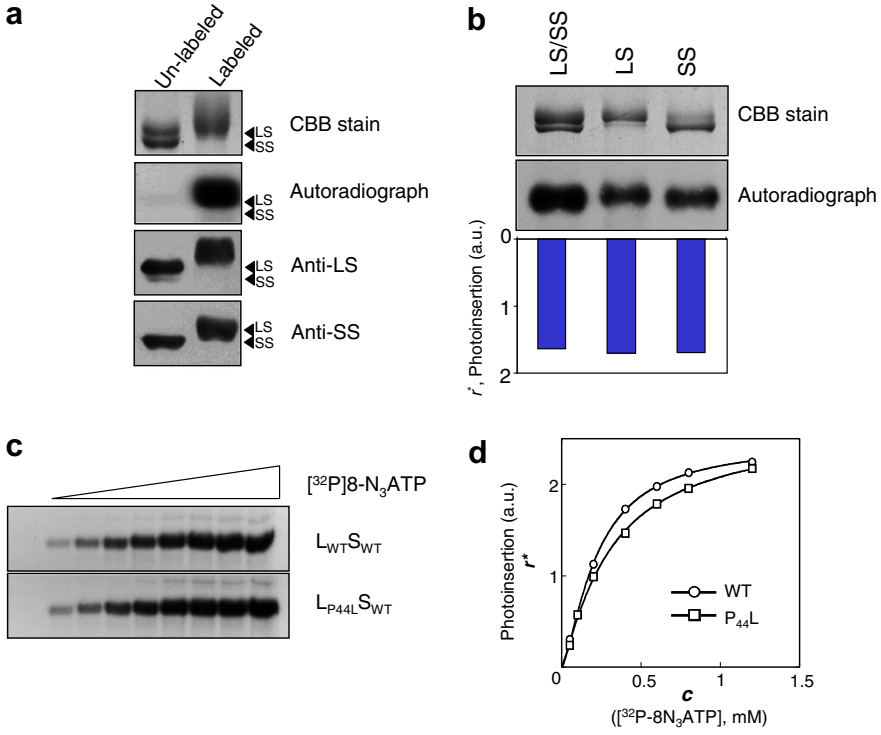

Fig. 4. Photo-affinity labeling of AGPases. (a) Wildtype AGPase was labeled in 1.2 mM of [α^{32}P]8-N_3ATP and 7 mM $MgCl_2$ with 5 mM 3-PGA and then separated by electrophoresis on 10% SDS–polyacrylamide gels. One gel containing 1.9 μg of AGPase per lane was stained with CBB R-250, dried and autoradiographed. The other gel containing 0.38 μg of AGPase per lane was used for immunoblot analysis by using anti-potato AGPase LS and SS antibodies. (b) Stoichiometry of ATP binding. Wildtype AGPase was labeled under the same condition as described above except that 0.2 mM [^{32}P]8-N_3ATP was used. The LS and SS were separated from each other using immobilized metal affinity chromatography (TALON) under the urea denaturing conditions. Following SDS–PAGE and autoradiography of the gel, photoinsertion (r^*) was calculated by normalizing the labeling intensities of the protein bands with respect to the intensities of the protein bands on CBB stained gel. a.u., arbitrary unit. (c) [α^{32}P]8-N_3ATP labeling of the wildtype ($L_{WT}S_{WT}$) and P44^{LS} mutant ($L_{P44L}S_{WT}$) AGPases. Enzymes (1.5 μg per lane) were labeled in 0–1.2 mM of [α^{32}P]8-N_3ATP, 7 mM $MgCl_2$, and 5 mM 3-PGA. D. The ATP binding curves of the wildtype (open circle) and $P_{44}L$ mutant (open square) AGPases. The labeling curve was plotted by using the modified Hill equation (Eq. (1a)). *c*, concentration of [α^{32}P]8-N_3ATP.

centration (0.4 mM) of [^{32}P]8-N_3ATP. More interestingly, the result in Fig. 4b showed that both the LS and SS were labeled with the ATP analog to similar extents, indicating that regardless of possession of catalytic activity both subunits interact with ATP molecules.

Since wildtype and $P_{44}L$ mutant showed significantly different apparent affinities for ATP (Table 2), we anticipated marked differences in the labeling profiles between the two enzymes. Photo-affinity labeling experiments were conducted with various concentrations of [α^{32}P]8-N_3ATP under activating conditions (Fig. 4c). Photoaffinity labeling of the AGPase subunits was saturating, suggesting that cross-linking of the azido analogs was specific. Interestingly, $L_{WT}S_{WT}$ and $L_{P44L}S_{WT}$ were labeled to nearly the same extent: the apparent labeling affinity constants (K_L) estimated from the saturation kinetics were 0.23 mM and 0.31 mM, respectively. The K_L value (0.23 mM) of the wildtype enzyme was very similar to the apparent catalytic affinity ($S_{0.5} = 0.19$ mM, Table 2). However, the K_L value (0.31 mM) of $L_{P44L}S_{WT}$ was significantly lower than the apparent catalytic affinity ($S_{0.5} = 0.68$ mM) although the value was slightly higher than that of wildtype. When the labeling intensities of the proteins were normalized with respect to the corresponding protein bands, the maximum levels of labeling were nearly identical for both enzymes ($R^*_{max} = 2.5$–2.6). This result was unexpected because the two enzymes showed significant differences in specific activities (28 U/mg for $L_{WT}S_{WT}$ versus 0.8 U/mg for $L_{P44L}S_{WT}$) as well as the apparent $S_{0.5}$ value for ATP. These results indicate that ATP binding (labeling) itself is only indirectly related to the apparent substrate affinity and catalytic activity of the enzyme.

3. Discussion

Our new host (*E. coli* EA345) and new expression plasmids (pSH275 and pSH228) facilitated and enhanced expression and purification of the various AGPases. Previous results (Salamone et al., 2000) showed that the homotetrameric AGPase expressed in AC70R1-504 suffered significant degradation in contrast to the intact enzyme obtained from BL21 cells which lacked the major protease activities *lon* and *ompT*. Moreover, the partially degraded enzyme showed reduced sensitivity to 3-PGA activation as compared to the intact enzyme prepared from BL21 cells. The new host, AGPase-deficient (*glgC*$^-$) EA345, lacks the major proteases (*lon* and *ompT*) as well as the endonuclease A (*endA*), which increases plasmid stability. A second major improvement was the development of new plasmid vectors for enzyme expression. The previous pair of plasmid vectors (pML7 and pML10) used different promoters, *recA::T7* and *tac::T7*, respectively. However, the new plasmids express the AGPase subunits under an identical *lac* promoter so that only one inducer such as IPTG can be used for over-expression of the proteins. The employment of this new host strain and plasmid vectors resulted in more reproducible expression of the various heterotetrameric AGPases.

The higher plant AGPases are responsible for the control and production of starch in the plastids of source leaves and sink tissues and organs such as stems (tubers) and seeds. Of the various tissue specific forms, the potato tuber (stem form) enzyme has been extensively studied due to its relative efficient recombinant expression and stability. The two LSs and two SSs, which make up the heterotetrameric potato enzyme, share significant sequence homology (53% identity and 73% similarity) indicating they originated from a common ancestral gene (Smith-White and Preiss, 1992; Jin et al., 2005). Results from biochemical-genetic studies have suggested that each subunit had distinct roles in enzyme function. The SS is the catalytic subunit based on its capacity to form an active homotetrameric enzyme, albeit with defective regulatory properties (Ballicora et al., 1995); while the LS plays an important role in specifying the allosteric regulatory properties of the heterotetrameric enzyme (Ballicora et al., 1995; Greene et al., 1996a,b, 1998; Laughlin et al., 1998; Kavakli et al., 2001; Crevillen et al., 2003). The LS also interact synergistically with the SS to affect the control of the heterotetrameric enzyme (Hwang et al., 2005). Co-expression study of each of the four LS isoforms with the single SS from *Arabidopsis* also showed that the LS somehow influences the substrate affinities of the enzyme (Crevillen et al., 2003). Although the LS lacks or displays little catalytic activity, its functionality can be ''resurrected'' by site-directed mutagenesis of two residues located at the N-terminal region (Ballicora et al., 2005). Hence, the subunit types are both catalytic and regulatory although to different extents (Cross et al., 2004).

In order to get further insights into the roles of the LS and its N-terminal region in enzyme function, we generated additional mutations within this region by site-directed mutagenesis of the six proline residues located within the first 66 residues of the N-terminal region (Fig. 2a). Proline residues in the primary sequence were selected for mutagenesis as this residue forms a 'hunchback' conformation and thus its replacement was likely to affect the regional conformation of this peptide domain (Reiersen and Rees, 2001). The N-terminal region structure of the LS (Fig. 2b) was modeled based on the juxtaposed comparison of the LS with the recently published structure of the potato tuber SS homotetramer (Ballicora et al., 2005; Jin et al., 2005). Although the homotetrameric AGPase for crystallography was not a natural form *in planta* and the enzyme structure was determined in the T state (inhibitor sulfate bound), it still provides important structure–function insights at the molecular level. Other than a 9 amino acid insertion (residues 20–28) near the N-terminus in the LS, the predicted structure of the N-terminal region of LS is very similar to that observed for the SS homotetramer.

Three of the six Pro mutations at positions 44, 52 and 66 had striking effects on enzyme function (Table 2). $P_{52}L$ and

P_{66}L showed the most dramatic changes in affecting enzyme regulatory properties although with widely opposing effects. As reported previously (Greene et al., 1996a,b; Hwang et al., 2005), P_{52}L showed down-regulatory properties, i.e. lower sensitivity (7-fold) to 3-PGA activation and increased sensitivity to Pi inhibition. This result is consistent with the results of mutagenesis of the bacterial enzymes near this position, i.e. A_{44}T and K_{39}E in *E. coli* (Meyer et al., 1993). In contrast, P_{66}L rendered the enzyme with increased sensitivity (~4-fold) to 3-PGA activation and lower sensitivity to Pi inhibition. The other four Pro mutations resulted in only minor increases in sensitivity to 3-PGA (P_{17}L) or moderate decreases in sensitivity to 3-PGA (P_{26}L, P_{44}L, and P_{55}L). Pi inhibition profiles were similar among these mutants. In the crystal structure of the potato SS homotetrameric enzyme (Jin et al., 2005), two adjacent effector anion binding sites are observed within the N-terminal region. Site 1 is bounded by $R39^{SS}$, $R51^{SS}$, and $K402^{SS}$ with $K439^{SS}$ and $D401^{SS}$ making a salt bridge interaction with $R39^{SS}$. Site 2 consists of $R51^{SS}$, $R81^{SS}$, $H82^{SS}$ and $Q312^{SS}$ and $R314^{SS}$. Except for the site 1 $R39^{SS}$ and $K439^{SS}$, these residues are conserved in both subunits types. Although the site 1 equivalent in the LS may bind effector anions poorly due to the lack of conservation of $R39^{SS}$ and $K439^{SS}$, mutagenesis of the LS's $K414^{LS}$ (equivalent to $K402^{SS}$) and $D413^{LS}$ (equivalent to $D401^{SS}$) down-regulates activation by 3-PGA (Greene et al., 1996a) suggesting that the effector anion binding site 1 in the LS is functional and is involved in the allosteric regulation of the heterotetrameric enzyme. As $P52^{LS}$ and $P66^{LS}$ lie within these two potential effector anion binding sites, the alterations in allosteric regulatory properties by mutations in $P52^{LS}$ and $P66^{LS}$ could decrease and increase the affinity to 3-PGA, respectively, by the LS and, in turn, the heterotetrameric enzyme. Alternatively, $P52^{LS}$ lies in a loop located close to the lysine residues ($K414^{LS}$ and $K440^{LS}$) responsible for the putative 3-PGA binding sites. The $P_{52}L^{LS}$ mutation may alter the loop structure such that it sterically blocks 3-PGA binding to $K414^{LS}$ and $K440^{LS}$. Either explanation together with the presence of multiple pyridoxal phosphate labeling sites in the LS (Ball and Preiss, 1994) indicates that this subunit binds effectors and is actively involved in specifying the allosteric regulatory properties of the heterotetrameric enzyme. Hence, the net allosteric regulatory properties of the heterotetrameric enzyme are not the result of the LS simply modulating the ability of the SS to bind effectors but, instead, a product of the allosteric properties of each subunit type (Hwang et al., 2005).

It is interesting that in addition to changing the allosteric regulatory properties the LS's N-terminal region also impacts the catalytic properties of the heterotetrameric enzyme. Cells expressing the P_{44}L mutation showed a drastic reduction in iodine staining indicating that the enzyme activity was severely compromised *in vivo* (Fig. 2c). Unlike other mutations that significantly affected the allosteric regulatory properties, kinetic analyses showed that the P_{44}L mutation resulted in a nearly catalytically inactive enzyme (Table 2). This mutation also led to reductions in the apparent affinities for ATP and Glc-1-P, resulting in the substrate catalytic efficiencies to be significantly lower compared to the wildtype enzyme. $P44^{LS}$ replaced with other amino acids showed properties similar to P_{44}L (Table 3). Thus, it is likely that both the structural involvement of Pro itself and its location are critical for conferring substrate affinities and catalytic rate properties of the enzyme.

The homologous residue to $P44^{LS}$ in the SS is $P34^{SS}$ (designated $P36^{SS}$ in Jin et al., 2005). $P34^{SS}$ is situated between the GGXGXRL loop region (residues 26–32) which participates in binding ATP (by specifically positioning the phosphates groups of ATP for catalysis) and the effector anion binding site 1 in the homotetrameric SS enzyme. In the unbound state, the GGXGXRL loop is located in the active site but is forced to move out of the active site to accommodate binding of ATP or ADP-glucose. It has been predicted that mutation at $P34^{SS}$, which is in the *cis* configuration, would cause conformational changes and thus significantly affect the interaction between the allosteric binding site and the GGXGXRL loop region (Jin et al., 2005). This idea implicates high possibility of alteration with respect to allosteric and/or catalytic properties. The $P44^{LS}$ in the LS is predicted to be in the same *cis*-isomeric form in our model (Fig. 2b). Unexpectedly, mutation at the residue shows no obvious changes in the CD spectra (Fig. 3), indicating the mutation does not significantly impact protein conformation. However, mutations at $P44^{LS}$ greatly reduce enzyme's responsiveness to major metabolic effectors such as 3-PGA, 2-PGA, PEP, and fructose-6-phosphate (Table 4) although affinity ($A_{0.5}$ or $I_{0.5}$) to 3-PGA or orthophosphate was only slightly changed. Thus, P44 in the LS is important not for allosteric regulation but for fold-activation of the enzyme. The P_{44}L mutation in the LS also significantly changes the catalytic properties of the enzyme: 3.6-fold and 7-fold decreases in the apparent affinities for ATP and Glc-1-P, respectively, and 36-fold reduction in the apparent catalytic rate. The relatively small effect on ATP binding by P_{44}L is also supported by our photoaffinity labeling studies with $[\alpha^{32}P]8\text{-}N_3ATP$. The wildtype LS binds this nucleotide at about the same efficiency as the wildtype SS (Fig. 4b). The P_{44}L substitution has little effect as the mutated AGPase is labeled just as efficiently as the wildtype AGPase. The apparent contradiction between binding affinity and the catalytic activity was also observed with the *Rhodobacter sphaeroides* AGPase mutant containing the R_{22}A mutation (Kaddis et al., 2004) which bound ATP but not in the proper orientation for catalysis.

Although the catalytic properties of the enzyme is influenced by the interaction of the two subunits, their individual contributions are not equal with the SS being the dominant player (Fu et al., 1998; Frueauf et al., 2003). Mutation of the SS metal binding $D145^{SS}$ which interacts with the ribose moiety of ATP drastically decreases the catalytic rate (40- to >24,000-fold) as well as substrate affinities (6-fold for ATP although no affect for ADP-glucose was observed) of the heterotetramer (Frueauf et al.,

2003). Interestingly, this study also showed that mutations at the homologous $D160^{LS}$ resulted in decreases in the substrate affinities toward ATP (2- to 3-fold) and ADP-glucose (3- to 5-fold). Catalytic activity was also lowered but only by 2- to 3-fold. It is interesting to note that when both metal binding residues are mutated, the resulting double mutant enzyme shows a decrease ATP affinity far greater than the sum of the net decreases specified by each mutant subunit (e.g. 33-fold decrease in $S_{0.5\ ATP}$ for $L_{D160N}S_{D145E}$ vs. 9-fold for the sum contributed by $L_{D160N}S_{WT}$ and $L_{WT}S_{D145E}$; 19-fold for $L_{D160E}S_{D145E}$ vs. 8-fold for the sum of $L_{D160E}S_{WT}$ and $L_{WT}S_{D145E}$). This result indicates that the interaction between both subunits is synergistic for the enzyme's affinity toward ATP. Likewise, subunit synergy is also evident for the net catalytic (specific) activity of the double mutant enzyme (Frueauf et al., 2003).

The catalytic mechanism of the *E. coli* and higher plant AGPases follows a sequential ordered *bi bi* kinetic model (Haugen and Preiss, 1979; Kleczkowski et al., 1993a,b). The bacterial enzyme initially displays half-site reactivity where only two out of the four identical subunits bind ATP and Glc-1-P (Haugen et al., 1976). This property indicates that the bacterial enzyme is not composed of functionally equivalent subunits but, instead, contains two non-equivalent subunit pairs (A_2B_2). Binding of ATP followed by Glc-1-P in the A subunits mediates a conformational change in B types (flip-flop model) enabling these subunits to bind substrates in an orderly sequence (Jin et al., 2005). Interestingly, the crystal structure of the higher plant SS homotetrameric enzyme shows that only two out of the four subunits contain bound ATP suggesting that the catalytically disabled LS of the higher plant enzyme may be functionally equivalent to the B subunits of the bacterial enzyme. However, our photoaffinity labeling studies indicate that even in the absence of Glc-1-P, both subunit types react with the substrate 8-azido-ATP to nearly identical efficiency (Fig. 4b). Hence, the proposed flip-flop model for the bacterial enzyme is not operational for the higher plant heterotetrameric enzyme although it could be applicable for the SS homotetramer.

The ability to bind ATP and the capacity to restore (partial) catalytic activity of the LS by mutagenesis indicates that a few mutations into the LS during evolution resulted in a significant loss of catalytic activity but the LS still retains essential roles for proper function of the heterotetrameric enzyme. In this regard the LS can be considered as a catalytic-disabled subunit, which, however, binds effectors and substrates and is likely to undergo conformational changes identical or similar to that exhibited by the SS during its catalytic cycle (substrate binding to product formation and release). As the enzyme's catalytic and allosteric regulatory properties are a product of synergy between the two subunit types, alterations in capacity of the LS to bind effectors and substrates as well to engage in a pseudo-catalytic cycle would influence the SS catalytic properties and, in turn, the heterotetrameric enzyme.

4. Conclusions

The results reported herein reaffirm the idea that the LS or its N-terminus is essential for specifying the allosteric properties of AGPase. In addition to this our results emphasize that the LS also plays significant roles in the catalysis of the AGPase heterotetramer. Mutations at $P44^{LS}$ greatly impaired the catalytic properties of the heterotetrameric enzymes. The $P44^{LS}$ is also important for enzyme activation (increase in the catalytic rate) by metabolites. More importantly, the LS, structurally analogous to the catalytic SS, binds ATP. The LS affects the net catalytic properties of the heterotetrameric enzyme by interacting cooperatively with the catalytic SS. To further understand its role in catalysis of the heterotetrameric enzyme, the LS ATP binding site is being explored.

5. Experimental

5.1. Primers and bacterial host cells

The oligonucleotide primers used in this study are summarized in Table 1. *Escherichia coli* ER 2566 [*F⁻λ⁻fhuA2 [lon] ompT lacZ::T7 gene1 gal sulA11 d(mcrC-mrr) 114::IS10 R(mcr-73::miniTn10-TetS)2 R(zgb-210::Tn10) (TetS) endA1 [dcm]*] was obtained from New England Biolabs and used to generate a *glgC* null mutant. This strain has several advantages over the AC70R1-504 cell (Ballicora et al., 1995) as it lacks both *lon* and *ompT* proteases, as well as endonuclease A. In order to generate a *glgC* null mutation by recombination, the promoter region (495 bp) of the *glgCAP* operon was amplified by polymerase chain reaction (PCR) using the primers 5′glgc S and 5′glgc AS, genomic DNA (15 ng) from *E. coli* ER2566, and *Pfu Turbo* DNA polymerase (Stratagene). Amplification conditions were for 30 cycles consisting of 95 °C for 30 s, 58 °C for 1 min, and 68 °C for 1 min. The promoter fragment was digested with *Sma*I and *Nco*I and cloned into the corresponding sites of pGEM58ZN (GenBank Accession No. AF310245). This plasmid was then cut with *Nco*I and *Hin*dIII and ligated with an *Nco*I/*Hin*dIII fragment (0.85 kb) containing the 5′ end of the *glgC* gene which was PCR amplified with primers glgc S and pyro7 as described above. The resulting plasmid contains the *glgC* promoter and partial *glgC* coding sequence. Bacteriophage lambda DNA (GenBank Accession No. NC_001416) was cut with *Nco*I/*Eco*RI and the resulting 0.72-kb fragment (from 44,249 bp to 44,973 bp) was cloned into the same restriction sites downstream of the *glgC* promoter to replace part of the *glgC* coding sequence. The *glgC* promoter-Δ*glgC*::[0.72-kb lambda DNA]-*glgC* 3′ coding sequence was then obtained by digestion with *Bam*HI and *Hin*dIII, made blunt with *Pfu* DNA polymerase, and cloned into the *Sma*I sites of pKO-3 (Link et al., 1997) to generate pSH53. The *glgC* null mutant was generated and screened as described in Link et al. (1997) with several modifica-

tions. Briefly, ER2566 cells were transformed with pSH53 and grown at 42 °C for 2 days on LB-agar plates containing 30 μg/mL chloramphenicol. Colonies were pooled and incubated at 30 °C for 18 h in a 50-ml LB liquid medium containing 5% w/v sucrose. This culture step was repeated three times using 1% v/v of inoculum into fresh media. The cells were then streaked on Kornberg plates (1.1% K_2HPO_4, 0.85% KH_2PO_4, 0.6% yeast extract, 0.5% glucose, 1.8% agar) and incubated at 37 °C for overnight. Colonies with a glycogen-deficient phenotype were picked after staining with iodine vapor. Cells were cured of plasmids by culturing them repeatedly without antibiotic selection and then selecting colonies which were unable to grow on LB containing 30 μg/mL chloramphenicol. PCR was performed with the primers 5′glgc S and pyro7 under the same amplification conditions as described above and the PCR product sequenced to confirm the deletion in the *glgC* gene. The resulting mutant strain was named EA345.

5.2. Prediction of protein structure

Secondary structure of the potato AGPase LS (Iglesias et al., 1993; Greene et al., 1996a,b; Hwang et al., 2004; Hwang et al., 2005) was predicted using the PSIPRED protein structure prediction server (McGuffin et al., 2000). Only the residues with greater than 50% confidence level were regarded valid for determination of the secondary structures. Three dimensional structure of the LS was modeled based on the structural and sequence homologies with the potato SS homotetramer (Jin et al., 2005). DeepView, the Swiss-PdbViewer (http://www.expasy.org/spdbv/) and POV-Ray, the ray-tracing software (http://www.povray.org/) were used for modeling the structure.

5.3. Site-directed mutagenesis

Site-directed mutations were introduced in the potato AGPase LS. The LS sequence was cloned in a modified pTrc99 plasmid (Amersham-Pharmacia Biotech) lacking the *lacI*^{q} sequence which was removed by digestion with *Pvu*II and *Nde*I. Mutagenesis was performed using a Quik Change Site-Directed Mutagenesis Kit (Stratagene) with the primers described in Table 1. The plasmid was amplified using 16 cycles at 95 °C for 30 s, 56 °C for 1 min, and 68 °C for 12 min.

5.4. Expression plasmids

In place of pML7 and pML10 (Ballicora et al., 1995; Salamone et al., 2000) two new expression plasmids, pSH275 and pSH228, were constructed to express the AGPase LS and the SS, respectively. Briefly, pSH275 was constructed from pQE30 (Qiagen) which contains a *ColE1* replicon and an ampicillin-resistance gene (*bla*) while pSH228 made from pML10 (Greene et al., 1998) has a p15A replicon, kanamycin resistance gene, *lacI*^{q} gene, and bacteriophage lambda Q gene. Production of the lambda Q proteins is necessary for EA345 cells to initiate transcription of *glgA* and *glgP* genes. Both plasmids are IPTG-inducible.

5.5. Culture conditions and enzyme purification

EA345 cells were transformed with pSH228 containing the wildtype recombinant SS. The cells were further transformed with plasmids containing the wildtype LS or the proline mutants. Three colonies from each combination were picked and inoculated into 50-ml of LB (plus 0.4% glucose) liquid media containing 200 mg/L penicillin G and 50 mg/L kanamycin. The cells were grown overnight at 37 °C with vigorous shaking. The seed culture was then used to inoculate fresh 1-L NZCYM liquid medium (10 g NZ-amine, 5 g yeast extract, 5 g NaCl, 2 g $MgSO_4 \cdot 7\ H_2O$, and 1 g casamino acid in 1 liter) containing the same concentrations of antibiotics as above. IPTG was added to the final concentration of 100 μM when the optical density at 600 nm of the culture reached 1.0–1.2. Induction of AGPase was performed at room temperature for 24 h with vigorous shaking. Cells were harvested and disrupted as described in Hwang et al. (2005). Purification of AGPase from crude cell extracts were performed according to the procedures modified from Hwang et al. (2005). The crude extract was fractionated on a DEAE-Sepharose Fast Flow (Amersham) column (bed volume: 25 ml) using a salt gradient of 0–0.5 M NaCl in buffer A (25 mM Hepes–NaOH, pH 7.5, 10% glycerol). The fractions containing AGPase activity were pooled and loaded onto a TALON™ metal affinity resin (BD Biosciences) column which was equilibrated with 0.5 M NaCl in buffer A. AGPase activity was eluted using 200 mM imidazole in buffer A. For further purification a hydrophobic interaction chromatography step was performed. Ammonium sulfate was slowly added to the AGPase fractions obtained from the IMAC chromatography to a final concentration of 1 M, which was then applied to a Butyl-Sepharose Fast Flow (10-ml of bed volume; Amersham) column. After washing with 10 bed volumes of 1 M ammonium sulfate in buffer A (25 mM Hepes–NaOH, pH 7.0, 10% glycerol), AGPase was eluted with a salt gradient (1–0 M ammonium sulfate in buffer A). AGPase fractions were selected after SDS–PAGE analysis and pooled together. Afterward, two volumes of saturated ammonium sulfate solution pre-chilled at 4 °C were slowly added to precipitate the proteins. After precipitation by centrifugation, the pellet was resuspended with 1 ml of buffer A and the protein solution dialyzed against 1-L of buffer A at 4 °C for 24 h. After clarification by centrifugation the pure enzyme preparation was aliquoted and stored at −80 °C until used for analysis.

5.6. Enzyme assay

Sodium [^{32}P]pyrophosphate and [^{14}C]glucose-1-phosphate were purchased from Perkin–Elmer (NEN) and ICN Pharmaceuticals, respectively. AGPase activities were

performed in the reverse pyrophosphorylase (Assay A) direction during enzyme purification. For kinetic characterization the activities were measured in the forward ADP-glucose synthesis (Assay B) direction. One unit (U) is defined as the amount of enzyme that produces 1 μmol of ATP or ADP-glucose for 1 min.

Assay A – [^{32}P]ATP formation was measured from [^{32}P]PPi and ADP-glucose. Reaction was performed at 37 °C in 0.2 ml of 100 mM Hepes–NaOH, pH 7.0, 7 mM $MgCl_2$, 3 mM DTT, 5 mM 3-PGA, 10 mM NaF, 0.4 mg/ml bovine serum albumin, 1 mM ADP-glucose, 1.5 mM NaPPi, 3×10^6 cpm/ml [^{32}P]NaPPi as described in Hwang et al. (2004).

Assay B – [^{14}C]ADP-glucose formation from [^{14}C]Glc-1-P was determined for all kinetic measurements. The reaction was performed at 37 °C in 0.1 ml of 100 mM Hepes–NaOH, pH 7.0, 7 mM $MgCl_2$, 3 mM DTT, 5 mM 3-PGA, 0.4 mg/ml bovine serum albumin, 0.15 U inorganic pyrophosphatase (Sigma), 1.5 mM ATP, 1.5 mM Glc-1-P, and [^{14}C]Glc-1-P (1000–1200 dpm/nmol) as described in Hwang et al. (2004). 3-PGA activation and inorganic phosphate experiments, varied concentrations of the effectors were added to the reaction mixture. For metabolite activation analysis, 4 mM of each metabolite was added to the reaction mixture instead of 3-PGA.

5.7. Protein measurement and immunoblot analysis

Measurement of protein concentration, SDS–PAGE, and immunoblot analysis were performed as described in Hwang et al. (2004).

5.8. Circular dichroism (CD) analysis

For CD analysis the enzyme's storage buffer (buffer A) was replaced with 50 mM ammonium bicarbonate (pH 7.5) by using a Performa gel filtration cartridge (Edge Biosystems) and then the enzyme was concentrated with a 30 K Nanosep® centrifugal device (Pall Life Sciences). The wildtype and variant AGPases at 2.2 μM were used for CD analysis with AVIV Stopped Flow CD Spectrometer (model 202SF; Protein Solutions, Inc.). Spectra were recorded from 300 to 200 nm at 25 °C and corrected for buffer contributions.

5.9. Labeling of AGPases with 8-azido-ATP

[α^{32}P]8-N_3ATP and non-isotopic 8-N_3ATP were purchased from Affinity Labeling Technologies, Inc. The purified AGPase preparation was desalted into 100 mM Hepes–NaOH (pH 7.0) using a Performa gel filtration cartridge (Edge Biosystems). Labeling reaction mixture contained 50 mM Hepes–NaOH (pH 7.0), 7 mM $MgCl_2$, 5 mM 3-PGA, and varying amounts of [α^{32}P]8-N_3ATP (0.4 mCi/μmol). Proteins were labeled using 400 mJ/cm^2 of UV light for 5 min at room temperature using a UV cross-linker (Ultra-Lum, Inc., UVC-508). Immediately after UV treatment one-half volume of the labeling stop buffer containing 150 mM Hepes–NaOH (pH 7.0), 9 mM DTT and 30% glycerol was added and the samples analyzed by SDS–PAGE (Hwang et al., 2004). For separation of the subunits from each other the labeled protein mixture (100 μg) was applied to a Ni-NTA column after mixing with 19 volumes of 6 M urea in the binding buffer (Qiagen) and incubating for 30 min at room temperature. Chromatography under denaturing condition was done according to the manufacturer's instructions. The SS proteins in the unbound flow-through fraction and the LS proteins in the eluted fractions were precipitated with 15% TCA. The subunit pellets were then resuspended in SDS–PAGE sample buffer and then analyzed by polyacrylamide gel electrophoresis. Gels were dried under vacuum and subjected to autoradiography. The intensities of the protein bands (CBB stained gels) and autoradiographic signals were scored by using the ImageJ ver.1.33 software (NIH) after scanning the gels and films with a KODAK image analysis system. The labeling signals were then normalized with respect to the intensities of the protein bands. The linear relationship between the band intensity and protein amount was confirmed by measuring the intensities of the bands of different amounts of the wildtype AGPase.

5.10. Kinetic characterization

The kinetic parameters were determined using the Hill equation (Bell and Bell, 1988)

$$v = \frac{V^*_{\max}[\mathrm{L}]^h}{K^h_s + [\mathrm{L}]^h} \quad (1)$$

In this equation, v represents the reaction rate, $V^*_{\max}$ the apparent maximal reaction rate, [L] the concentration of the ligand (substrate or Pi), K_s the reaction constant ($S_{0.5}$ or $I_{0.5}$), and h the Hill coefficient (nH). The $S_{0.5}$ values for ATP, Mg^{2+}, and Glc-1-P correspond to the substrate levels required for 50% maximal activity in the presence of saturating 3-PGA.

Our preliminary results showed that even in the absence of the metabolic activator some of the potato AGPase variants have significant levels of enzyme activity. Thus a modified form of the Hill equation was used for calculation of $A_{0.5}$.

$$v = v_o + \frac{(V^*_{\max} - v_o)[\mathrm{A}]^h}{A^h_{0.5} + [\mathrm{A}]^h} \quad (2)$$

In this equation v_o represents the initial reaction rate in the absence of 3-PGA and [A] the concentration of 3-PGA. The $A_{0.5}$ value corresponds to the 3-PGA concentration required for 50% maximal activation of enzyme.

The K_s ($S_{0.5}$ or $I_{0.5}$) and $A_{0.5}$ values were determined by fitting the experimental data from Assay B to Eqs. (1) and (2), respectively, with the aid of Kaleidagraph (Synergy Software, Reading, PA). For inhibition analysis, the $I_{0.5}$ value corresponding to the Pi concentration required for 50% inhibition was calculated from the fractional inhibi-

tion of enzyme activities plotted vs. Pi concentrations (0–10 mM) by fitting the data to Eq. (1) as above.

For analysis of the substrate (ATP) binding affinity through the labeling experiment the modified Eq. (1) (Eq. (1a)) and the modified Scatchard equation were used (Eq. (3)).

$$r^* = \frac{R^*_{\max} c^h}{K^h_L + c^h} \tag{1a}$$

$$\frac{r^*}{c} = K_L(n - r^*) \tag{3}$$

where r^* represents the normalized labeling intensity equivalent to the bound (labeled) [^{32}P]ATP, $R^*_{\max}$ the maximal intensity (normalized), h the Hill coefficient, c the concentration of free [^{32}P]8-N_3ATP, K_L the equilibrium binding (labeling) constant, and n the number of binding sites.

Acknowledgements

This work was supported by Department of Energy Grant No. DE-FG02-96ER20216 and falls under the purview of the Hatch Regional NC-1142 Project. We thank Dr. Lisa Gloss for expert assistance with CD spectroscopy.

References

Ball, K., Preiss, J., 1994. Allosteric sites of the large subunit of the spinach leaf ADP-glucose pyrophosphorylase. J. Biol. Chem. 269, 24706–24711.

Ballicora, M.A., Laughlin, M.J., Fu, Y., Okita, T.W., Barry, G.F., Preiss, J., 1995. Adenosine 5′-diphosphate-glucose pyrophosphorylase from potato tuber. Significance of the N-terminus of the small subunit for catalytic properties and heat stability. Plant Physiol. 109, 245–251.

Ballicora, M.A., Fu, Y., Nesbitt, N.M., Preiss, J., 1998. ADP-Glucose pyrophosphorylase from potato tubers. Site-directed mutagenesis studies of the regulatory sites. Plant Physiol. 118, 265–274.

Ballicora, M.A., Iglesias, A.A., Preiss, J., 2004. ADP-glucose pyrophosphorylase: a regulatory enzyme for plant starch synthesis. Photosynth. Res. 79, 1–24.

Ballicora, M.A., Dubay, J.R., Devillers, C.H., Preiss, J., 2005. Resurrecting the ancestral enzymatic role of a modulatory subunit. J. Biol. Chem. 280, 10189–10195.

Bell, J.E., Bell, E.T., 1988. Proteins and Enzymes. Prentice-Hall, Englewood Cliffs, NJ, pp. 465–470.

Crevillen, P., Ballicora, M.A., Merida, A., Preiss, J., Romero, J.M., 2003. The different large subunit isoforms of *Arabidopsis thaliana* ADP-glucose pyrophosphorylase confer distinct kinetic and regulatory properties to the heterotetrameric enzyme. J. Biol. Chem. 278, 28508–28515.

Cross, J.M., Clancy, M., Shaw, J.R., Greene, T.W., Schmidt, R.R., Okita, T.W., Hannah, L.C., 2004. Both subunits of ADP-glucose pyrophosphorylase are regulatory. Plant Physiol. 135, 137–144.

Doan, D.N., Rudi, H., Olsen, O.A., 1999. The allosterically unregulated isoform of ADP-glucose pyrophosphorylase from barley endosperm is the most likely source of ADP-glucose incorporated into endosperm starch. Plant Physiol. 121, 965–975.

Frueauf, J.B., Ballicora, M.A., Preiss, J., 2003. ADP-glucose pyrophosphorylase from potato tuber: site-directed mutagenesis of homologous aspartic acid residues in the small and large subunits. Plant J. 33, 503–511.

Fu, Y., Ballicora, M.A., Preiss, J., 1998. Mutagenesis of the glucose-1-phosphate-binding site of potato tuber ADP-glucose pyrophosphorylase. Plant Physiol. 117, 989–996.

Gomez-Casati, D.F., Iglesias, A.A., 2002. ADP-glucose pyrophosphorylase from wheat endosperm. Purification and characterization of an enzyme with novel regulatory properties. Planta 214, 428–434.

Greene, T.W., Chantler, S.E., Kahn, M.L., Barry, G.F., Preiss, J., Okita, T.W., 1996a. Mutagenesis of the potato ADP-glucose pyrophosphorylase and characterization of an allosteric mutant defective in 3-phosphoglycerate activation. Proc. Natl. Acad. Sci. USA 93, 1509–1513.

Greene, T.W., Woodbury, R.L., Okita, T.W., 1996b. Aspartic acid-413 is important for the normal allosteric functioning of ADP-glucose pyrophosphorylase. Plant Physiol. 112, 1315–1320.

Greene, T.W., Kavakli, I.H., Kahn, M.L., Okita, T.W., 1998. Generation of up-regulated allosteric variants of potato ADP-glucose pyrophosphorylase by reversion genetics. Proc. Natl. Acad. Sci. USA 95, 10322–10327.

Haugen, T.H., Preiss, J., 1979. Biosynthesis of bacterial glycogen. The nature of the binding of substrates and effectors to ADP-glucose synthase. J. Biol. Chem. 254, 127–136.

Haugen, T.H., Ishaque, A., Preiss, J., 1976. Biosynthesis of bacterial glycogen. Characterization of the subunit structure of *Escherichia coli* B glucose-1-phosphate adenylyltransferase (EC 2.7.7.27). J. Biol. Chem. 251, 7880–7885.

Hwang, S.K., Salamone, P.R., Kavakli, H., Slattery, C.J., Okita, T.W., 2004. Rapid purification of the potato ADP-glucose pyrophosphorylase by polyhistidine-mediated chromatography. Protein Expression Purif. 38, 99–107.

Hwang, S.K., Salamone, P.R., Okita, T.W., 2005. Allosteric regulation of the higher plant ADP-glucose pyrophosphorylase is a product of synergy between the two subunits. FEBS Lett. 579, 983–990.

Iglesias, A.A., Barry, G.F., Meyer, C., Bloksberg, L., Nakata, P.A., Greene, T., Laughlin, M.J., Okita, T.W., Kishore, G.M., Preiss, J., 1993. Expression of the potato tuber ADP-glucose pyrophosphorylase in *Escherichia coli*. J. Biol. Chem. 268, 1081–1086.

Jin, X., Ballicora, M.A., Preiss, J., Geiger, J.H., 2005. Crystal structure of potato tuber ADP-glucose pyrophosphorylase. EMBO J. 24, 694–704.

Kaddis, J., Zurita, C., Moran, J., Borra, M., Polder, N., Meyer, C.R., Gomez, F.A., 2004. Estimation of binding constants for the substrate and activator of *Rhodobacter sphaeroides* adenosine 5′-diphosphate-glucose pyrophosphorylase using affinity capillary electrophoresis. Anal. Biochem. 327, 252–260.

Kavakli, I.H., Park, J.S., Slattery, C.J., Salamone, P.R., Frohlick, J., Okita, T.W., 2001. Analysis of allosteric effector binding sites of potato ADP-glucose pyrophosphorylase through peverse genetics. J. Biol. Chem. 276, 40834–40840.

Kleczkowski, L.A., Villand, P., Luthi, E., Olsen, O.A., Preiss, J., 1993a. Insensitivity of barley endosperm ADP-glucose pyrophosphorylase to 3-phosphoglycerate and orthophosphate regulation. Plant Physiol. 101, 179–186.

Kleczkowski, L.A., Villand, P., Preiss, J., Olsen, O.A., 1993b. Kinetic mechanism and regulation of ADP-glucose pyrophosphorylase from barley (*Hordeum vulgare*) leaves. J. Biol. Chem. 268, 6228–6233.

Laughlin, M.J., Chantler, S.E., Okita, T.W., 1998. N- and C-terminal peptide sequences are essential for enzyme assembly, allosteric, and/or catalytic properties of ADP-glucose pyrophosphorylase. Plant J. 14, 159–168.

Link, A.J., Phillips, D., Church, G.M., 1997. Methods for generating precise deletions and insertions in the genome of wild-type *Escherichia coli*: application to open reading frame characterization. J. Bacteriol. 179, 6228–6237.

McGuffin, L.J., Bryson, K., Jones, D.T., 2000. The PSIPRED protein structure prediction server. Bioinformatics 16, 404–405.

Meyer, C.R., Ghosh, P., Nadler, S., Preiss, J., 1993. Cloning, expression, and sequence of an allosteric mutant ADP-glucose pyrophosphorylase from *Escherichia coli* B. Arch. Biochem. Biophys. 302, 64–71.

Preiss, J., 1984. Bacterial glycogen synthesis and its regulation. Annu. Rev. Microbiol. 38, 419–458.

Preiss, J., Ball, K., Smith-White, B., Iglesias, A., Kakefuda, G., Li, L., 1991. Starch biosynthesis and its regulation. Biochem. Soc. Trans. 19, 539–547.

Reiersen, H., Rees, A.R., 2001. The hunchback and its neighbours: proline as an environmental modulator. Trends Biochem. Sci. 26, 679–684.

Salamone, P.R., Greene, T.W., Kavakli, I.H., Okita, T.W., 2000. Isolation and characterization of a higher plant ADP-glucose pyrophosphorylase small subunit homotetramer. FEBS Lett. 482, 113–118.

Salamone, P.R., Kavakli, I.H., Slattery, C.J., Okita, T.W., 2002. Directed molecular evolution of ADP-glucose pyrophosphorylase. Proc. Natl. Acad. Sci. USA 99, 1070–1075.

Slattery, C.J., Kavakli, I.H., Okita, T.W., 2000. Engineering starch for increased quantity and quality. Trends Plant Sci. 5, 291–298.

Smith-White, B.J., Preiss, J., 1992. Comparison of proteins of ADP-glucose pyrophosphorylase from diverse sources. J. Mol. Evol. 34, 449–464.